Supporting Information

Eikeset et al. 10.1073/pnas.1212593110

SI Text

SI Text consists of two main sections: *SI Materials and Methods* and *SI Results*. In the first section, we describe the biological and economic components of the bioeconomic model, including a description of the data used to parameterize the model (Table S1). At the end of *SI Materials and Methods*, we discuss model limitations. In *SI Results*, we show in greater depth the emerging properties of the historic fishing scenario that may give rise to an evolutionary cost. Also, we investigate the implications of alternative discount rates for deriving optimal harvest control rules (HCRs). Furthermore, we probe into the robustness of our results. Simulating different levels of constant fishing mortality rates (0.2–0.8 y^{-1}), we evaluate the impact of changing the minimum size limit, assuming a constant price, weight-dependent price, and, finally, changing the coefficient of genetic variation (i.e., evolvability) of the genetic life-history traits.

SI Materials and Methods: Model and Data Description

Biological Model. The biological model is an individual-based model that uses the framework developed in ref. (1). This model combines quantitative genetics with ecological processes taking place at the individual level to derive knowledge on how fishing pressure progressively affects the stock at the population level. The genetic component of this model allows individuals to adapt to the selection pressure brought about by harvesting. The individual-based model follows about 50,000 superindividuals (2, 3). All models results, such as spawning stock biomass (SSB) and catch, are given for a population that has been scaled up by a factor of 100,000 to recreate realistic stock levels. Parameter values for our model (Table S1) are based on published sources, data collected by the Norwegian Institute of Marine Research (IMR), Knipovich Polar Research Institute of Marine Fisheries and Oceanography (PINRO), and the Norwegian Directorate of Fisheries, and survey data made available through the International Council for the Exploration of the Sea (ICES). This model has been developed and calibrated for the Northeast Arctic (NEA) cod stock in ref. 4. A similar model was used in ref. 5 for the same stock, without considering any evolutionary dynamics.

Evolutionary dynamics. This section describes first how we model the phenotypic expression of the genetic traits for individual maturation tendency, growth, and reproductive investment; second, how we introduce the distribution of the evolving genetic traits in the initial population; and finally, how the traits are inherited by offspring. Each genetic trait value z_G (denoted by subscript G) has a corresponding phenotypic trait value z_P (denoted by subscript P), with a genetic variance $\sigma^2_{z,G}$ and phenotypic variance $\sigma^2_{z,P}$. At the population level, we assume phenotypic variance to be the sum of the genetic and environmental variance ($\sigma^2_{z,P} = \sigma^2_{z,G} + \sigma^2_{z,E}$). Based on quantitative genetics (6), each trait has a heritability, $h^2_z = \sigma^2_{z,G}/\sigma^2_{z,P}$, which allows us to calculate the environmental variance $\sigma^2_{z,E} = \sigma^2_{z,G}(h_z^{-2} - 1)$ for each trait in the initial population (where $\sigma^2_{z,G}$ is empirically determined for each trait; see below). This environmental variance was then subsequently kept constant through time. The four considered quantitative genetic traits are the maturation tendency by a probabilistic maturation reaction norm (PMRN): (*i*) slope $z_G = s_G$ and (*ii*) intercept $z_G = i_G$; and (*iii*) growth capacity $z_G = g_G$ and (*iv*) reproductive investment, given by the gonadosomatic index $z_G = GSI_G$. In the initial population, the genetic traits are assumed to be normally distributed with mean initial trait values and genetic variances determined by the coefficient of genetic variation $CV_{z,G}$, both based on empirical data (Table S1). The genetic traits are expressed phenotypically by random draws from a normal distribution with means equal to the respective genetic trait (see Table S1 for initial values), with the corresponding environmental variances σ^2_E. We examined an evolutionary and a nonevolutionary version of the model, each modeling their respective population of individuals to compare a population that has the propensity to evolve with a population that does not evolve. First, the nonevolutionary model was calibrated to accomplish a match with data on NEA cod phenotypic growth, biomass, and age and length at maturation for the period 1932–1950 (4). For the nonevolving population, which is only driven by ecological processes, the $CV_{z,G}$ by definition equals zero. In the evolving population, $CV_{z,G}$ was determined by matching trends in age and length at maturation over a 74-y period (1932–2005); for all four evolving traits, these were then varied to determine the amount of evolution needed to match the maturation trends for 1932–2005. Based on previous models, the range of evaluated $CV_{z,G}$ was between 0% and 12% (1, 7–9). All possible combinations were systematically evaluated and ranked by log-likelihood. The combination that ranked best was consequently selected and used to define the $CV_{z,G}$ values for each trait.

Offspring inherited genetic trait values from their parents by drawing randomly from normal distributions with means equal to the midparental genetic trait values (i.e., the arithmetic mean trait value of the two parents) and variances equal to half the variance for a given genetic trait in the initial population (thus assuming a constant recombination–segregation–mutation kernel) (1, 10). After the initial year (e.g., the first year in the simulation), genetic means, heritabilities, and the trait distributions could change freely as determined by the processes of maturation, somatic growth, reproduction, natural mortality, and harvesting mortality. These processes were applied sequentially in each year to all individuals.

Maturation, growth, reproduction, and mortality. Each year, the probability p_m that an immature individual will mature is described by a PMRN (11, 12); this is a function of the individual's length l and age a and given by $p_m = [1+\exp(-(l - l_{p50,a})/v)]^{-1}$. The length $l_{p50,a}$ is where the maturation probability p_m is equal to 50% at age a, as given by $l_{p50,a} = i_P + s_P a$, with a phenotypic intercept i_P and slope s_P. The parameter v is determined by the lower bound probability p_l (25%) and the upper bound probability p_u (75%) of the maturation envelope (1, 4), together with the PMRN width w, as given by $v = w/\ln\frac{p_l^{-1}-1}{p_u^{-1}-1}$.

To reflect density dependence in growth brought about by changes in abundance, and consequently competition and resource availability, we used an estimated relationship of phenotypic growth $g_{P,D,t} = g_{P,t}\exp(-xB_t)$, depending on total stock biomass B_t in year t. The hypothetical length increment where biomass B_t is zero is referred to as the maximum growth increment, and x is the strength of density dependence reducing growth relative to this maximum. For this estimation (Table S1), derived in detail in ref. 4 and used in ref. 5, we used data on annual growth increments and biomass for the period 1978–2009, obtained from survey data and stock assessment (4, 13). The parameters were estimated by regressing log-transformed mean annual growth increments for ages 0–5 y in the winter survey against total biomass and other covariates ($R^2 = 73\%$) (4). For the immature individuals, denoted by a superscript I, the body length in a given year depends on the length in the previous year and the growth increment in that year, $l^I_t = l^I_{t-1} + g_{P,D,t-1}$. Mature individuals, denoted by a superscript M, also allocate re-

sources to reproduction, depending on the reproductive investment; this is given by the phenotypic gonadosomatic index GSI_P and a conversion factor γ, needed to account for the higher energy content of gonadic tissue relative to somatic tissue (14, 15). Consequently, the length of a mature individual is given by $l_t^M = 3(l_{t-1}^M + g_{P,D,t-1})/(3+\gamma GSI_{P,t-1})$. An individual female's fecundity f is determined by its length l and gonadosomatic index phenotype GSI_P and given by $f = kl^j GSI_P D$, where D is the weight-specific packing density of oocytes (16), and k and j are allometric constants relating body length to body mass. The gonad weight at a given age can be calculated from fecundity by dividing it by the weight-specific packing density (shown in Fig. S1). An individual's probability to mate is proportional to its gonad mass, where large gonads due to larger body size and/or gonadosomatic index result in a higher production of gametes (eggs and sperm), and therefore in the production of more offspring. In our model, sex was assigned randomly at birth at a 1:1 primary sex ratio. Atlantic cod are batch spawners and so may mate with several different partners (17, 18). We therefore assumed mating to be random with replacement.

The individuals can die from natural or fishing mortality. In our model, natural mortality originated from three sources: newborn mortality, cost of growth, and a constant background natural mortality. The density-dependent newborn mortality was modeled by using an estimated Beverton–Holt stock-recruitment relationship (19) from virtual population analysis (VPA) data (20, 21). Recruitment depends on SSB_t in year t and sea surface temperature SST_t, reflecting the impact of climate. The sea surface temperature stretches from the Kola meridian transect (33°50' E, 70°50' N to 72°50' N) and has been shown to be a good indicator for recruitment for NEA cod (22–25). The expected number $R_{3,t}$ of recruits at age 3 y is then given by $R_{3,t+3} = c_0 SST_t + (c_1 SSB_t/(1+c_2 SSB_t))$, where c_0, c_1, and c_2 are statistically estimated parameters ($R^2 = 58.9\%$). The two density-dependent parameters c_1 and c_2 were scaled to the modeled population (Table S1). Annual temperature data from 1932 to 2005 was fed into the modeled stock-recruitment relationship, and after 2006 we used the average from 1995 to 2005. In this stock-recruitment model, we ignore cannibalism, even though it has been shown to be important for natural mortality in young age classes (24, 26). We found the expected number $R_{0,t}$ of newborn recruits by back-calculating the predicted number of 3-y olds, assuming an annual total natural mortality probability equal to 0.2 y^{-1}, as conventionally done for this stock in assessment (21). The survival probability of the offspring of a given spawning pair was equal to $R_{0,t}$ divided by the total fecundity of the spawning population.

The second source of mortality, the growth–survival tradeoff, accounts for less energy available for maintenance (27, 28) and lower survival as growth increases, which may be a result of, for example, risky foraging behavior (29, 30). We therefore included a tradeoff between an individual's survival and genetic growth capacity g_G through the extra mortality probability $m_g = g_G/g_{max}$, where g_{max} is the maximal genetic growth increment at which the survival probability drops to zero, and determines the strength of this tradeoff. The parameter g_{max} is a priori unknown and has been determined in a nonevolutionary model to imitate the stock demographically from 1932 to 1950 (4), by varying g_{max} from 50 to 200 cm, in steps of 5 cm, resulting in 31 evaluated combinations. This grid covered the range of values being assumed in published versions of this model (1, 7). Comparing model predictions with time-series data on phenotypic growth, biomass, and mean age and length at maturation for the period 1932–1950, the growth–survival tradeoff g_{max} was determined by log-likelihood (Table S1). Together, the background natural mortality and the additional mortality resulting from the growth–survival tradeoff produced annual natural mortality probabilities m equal to 0.18, as assumed by ICES in its VPA analyses (Table S1).

As is the case for NEA cod, harvesting was implemented in the model separately in the feeding grounds and spawning grounds. In the feeding grounds, harvesting was size-selective with minimum size limits within the range recorded for NEA cod from the 1980s onward (31). In the spawning grounds, only mature individuals were harvested, and there was no minimum size limit. Due to annual spawning migration out of the feeding grounds for approximately one-quarter of the year, the harvest probability of mature fish on the feeding grounds was $1-(1-p_0)^{3/4}$, where p_0 is the harvest probability for the immature fish.

Economic Model. To calculate the welfare effects of harvesting, we first specify the harvest function; second, specify the profit function; third, derive a procedure for allocating fishing quotas; and fourth, derive the demand function. All of these functions have been estimated and derived in detail in ref. 32 and used in ref. 5. Furthermore, we specify the objective functions to derive an optimal HCR.

Harvest function. Following refs. 33 and 34, the harvest function of vessel i in year t is given by a Cobb–Douglas production function $h_{it} = qB_t^{\alpha} e_{i,t}^{\beta}$, where q is a catchability coefficient, B_t is the amount of total stock biomass, and $e_{i,t}$ is fishing effort. In our model, effort is defined as the number of days a boat is fishing cod north of 62° N, multiplied by the size (given in gross tonnage) of the boat. The stock–output elasticity α and effort–output elasticity β describe how harvest changes when the respective inputs, biomass, and effort change.

Profit function. The cost data for each vessel contains expenses made for labor wages and shares to crew; social expenses (i.e., payroll-related expenses, such as employer contributions to pension and the employer portion of social security tax); fuel and lubrication oil; bait, ice, salt, and packaging; food expenses to crew, as well as maintenance on vessel, maintenance and investment on gear, insurance on vessel, other insurances, depreciation on vessel, and other operating expenses (35). In total, there are 11 cost components, which are indexed k = 1 ... 11. Total costs incurred by vessel i in year t are given by the vector of nominal cost components $C_{ik,t}$, which are subsequently corrected for inflation using the Producer Price Index (PPI). We calculate the part of the total costs incurred for catching cod by the share of days vessel i spends on catching cod in the total number of days vessel i is fishing at sea. Using index j to enumerate all eight fish species caught (with cod being j = 8) and denoting the number of days in year t that vessel i catches species j by $D_{ij,t}$, the total number of days vessel i spends catching fish in year t is equal to $\sum_{j=1}^{8} D_{ij,t}$. Therefore, the costs attributed to catching cod by vessel i in year t are $C_{i,t} = (D_{i8,t}\sum_{k=1}^{11} c_{ik,t})/(PPI_t \sum_{j=1}^{8} D_{ij,t})$.

We empirically determine which fraction of the costs of fishing per boat $C_{i,t}$ comprise fixed and variable costs by estimating $C_{i,t} = c_f + c_v e_{i,t}$, where c_f can be interpreted as fixed costs, and c_v are variable costs. Multiplying the catch $h_{i,t}$ of vessel i with the price of cod P_t yields the revenue $P_t h_{i,t}$ of vessel i. The profit $\pi_{i,t}$ of vessel i is then given by offsetting this revenue with the costs of vessel i and given by $\pi_{i,t} = P_t h_{i,t} - c_f - c_v e_{i,t}$.

Issuing individual quotas. Harvest quotas could in principle be allocated through a market mechanism, such as an auction, or handed out by the government to the boat owners. It is not clear a priori what the most efficient allocation (or market outcome) is, because the size of the quota and number of quotas can vary. Each boat faces a fixed cost, but is harvesting less efficiently when the size of the quota per boat increases, determined by the estimated effort–output elasticity (parameter β in Table S1). For each year t, we identify an optimal number n_t^* of vessels harvesting an optimal number e^* of tonnage days for a given total allowable catch (TAC) and total stock biomass (for details, see ref. 32), where $n_t^* = H_t q^{-1} e^{*-\beta} B_t^{-\alpha}$.

Demand function. The NEA cod fishery contributes a large part of the world's cod landings and therefore affects the international

market price for cod. To describe this relationship, we use a linear demand function, $P_t = b_0 - b_1 H_t$, where P_t is the price for cod in year t, H_t is the total harvested biomass in year t (as determined by the TAC), and b_0 and b_1 are parameters. The inverse price elasticity is estimated to be 0.5, i.e., if the supply of cod increases by 1%, the world price drops by 0.5% (32). Using the average kilogram price in the period 1998–2007 [in 2000 Norwegian kroner (NOK)] of 12.59 NOK, and the average landing of 527,800 tonnes allows us to solve for b_0 and b_1 (Table S1).

Objective function and HCR. Each year, the NEA cod fishery generates economic profits for the fishing fleet, given by Π_t. Finding the maximum economic yield requires us to maximize the NPV of the fishery over T years, as given by $\text{NPV} = \sum_{t=0}^{T} \Pi_t (1/(1+\delta))^t$, where δ is the discount rate.

The HCR implemented for the NEA cod fishery in 2004 translates precautionary reference points into a management plan (21, 36). Below these reference points, the stock is at risk for being harvested unsustainably. The implemented HCR for the NEA cod in 2004 consists of two parameters (37, 38): a maximum fishing mortality F_{pa} is followed if the spawning stock biomass level is above the precautionary biomass level B_{pa}; below this biomass level, the fishing mortality decreases linearly to the origin, i.e., fishing mortality is zero at a biomass level of zero.

Here, we generalize a HCR with two parameters (Fig. 1*B*), which can be compared with the implemented management plan. If the SSB is between zero and $B_{\max}$, the instantaneous fishing mortality for the given year is given by $F_{\max}\text{SSB}/B_{\max}$. If the SSB is larger than $B_{\max}$, the fishing mortality is equal to $F_{\max}$. The current HCR is therefore recovered as a special case when $B_{\max} = B_{\text{pa}}$ and $F_{\max} = F_{\text{pa}}$. In our model, we vary the parameters in the HCR over a wide range of values, not constraining them to existing precautionary reference points. We search for the combination of parameter values $B_{\max}$ and $F_{\max}$ that deliver the best results for the objective function (maximize the net present value of fleet profits) and identify those as optima. The grid for the parameters covered 4,141 different HCRs. The parameter $B_{\max}$ was varied from 0 to 800,000 tonnes in steps of 20 tonnes, and the instantaneous fishing mortality $F_{\max}$ was varied from 0.2 to 1.2 y^{-1} in steps of 0.01 y^{-1}. Our model is individual-based, and for some of these HCRs, fishing could make the abundance very low. To avoid stochastic effects at low abundances, we therefore set a threshold below which the population was classified as extinct (at 20 modeled mature superindividuals) (3, 4). The computations were completed on Abel, a computer cluster with 10,000+ cores at the Research Computing Services at the University of Oslo.

Model Limitations. As with all models, our bioeconomic model has limitations and involves simplifications. A few assumptions merit special attention here. First, we assume an initial 1:1 sex ratio, although it has been shown that the sex ratio has fluctuated over time in this cod stock (39). Second, we assume no sexual selection, although it is possible that sexual selection may influence the evolutionary changes in life-history traits (40–42). Third, we do not include genetic correlations between the life-history traits describing maturation tendency, growth capacity, and reproductive investment (4). Fourth, we assume a constant minimum size limit that determines the harvestable biomass (Table S1), implicitly assuming knife-edge selectivity (19, 43), which may not be fully realistic. Although our size limit is based on data, the size selectivity has varied over the considered time period and across vessels since 1932 (for a sensitivity analysis with respect to minimum size limit, see Table S5). Fifth, the shape of the HCR we are considering is constrained by two parameters, reflecting the current management plan. Investigating completely different shapes or considering HCR parameters that change over time is an interesting avenue for further research. Sixth, we focused on the fishery in the stock's feeding grounds and kept the fishing mortality at observed levels in the stock's spawning grounds; we did this because we wanted to mimic the historic selection pressure on the mature fish, while parsimoniously asking what can be changed for the trawler fleet in the Barents Sea. This assumption could be changed, and the next step would be to derive an optimal HCR for each of these fisheries.

SI Results

Historic Fishing Pressure. Table S4 shows the harvesting properties for the scenario of historic fishing pressure (i.e., high fishing mortality) presented in Fig. 2. The evolutionary model delivers lower TAC, total biomass from age 3 y, and lower NPV, whereas the SSB is slightly higher compared with the nonevolutionary model.

In Fig. S1 we show the life-history changes in the scenario of historic fishing pressure, corresponding to Figs. 2 and 3. Genetic adaptations caused by fishing pressure lead to higher reproductive investment (Fig. S1*A*) and genetic growth (Fig. S1*B*). As a result, the evolving population has consistently larger gonad weight (Fig. S1*C*) and higher phenotypic growth (Fig. S1*D*). Due to evolutionary changes, the ratio between spawning stock biomass and total biomass changes over time because of a change in maturation schedule (Fig. S4), and this may have implications for stock assessment and the target reference points that are used for management.

Alternative Discount Rates. Table S2 presents optimal HCR derived for alternative discount rates. As expected, higher discount rates lead to slightly higher fishing mortality, even though only marginally. This finding may seem surprising, but happens because larger catches result in lower prices, and hence profits. At a certain point, the resulting profit loss from lower prices outweighs the profit gain resulting from catching more fish, irrespective of the discount rate (5).

Alternative Scenarios with Constant Fishing Mortalities. ***Constant and weight-dependent prices.*** We probe the robustness of our results by varying the fishing mortality under alternative assumptions and investigating how this influences the effects of evolutionary changes. First, as a theoretical exercise, we assume that sales prices are independent of the total catch and the price is constant; this is clearly not realistic for the NEA cod fishery, but certainly the case for many other fisheries. As a constant price, we use the inflation-corrected average kilogram price in the period 1998–2007 of 12.59 NOK. Second, in addition, we assume that sales prices are weight-dependent, i.e., the price that can be obtained per kilogram of cod rises with the weight of the fish; we found little evidence that this is actually the case for the fleet of trawlers we are considering here, but it may be relevant for other vessel types, notably smaller coastal vessels. As a theoretical benchmark, we can rely on the minimum prices from the Norwegian fishermen's sales organization (44). The prices for the different weight classes are as follows. Cod that is heavier than 6.5 kg yields 17 NOK per kilogram. Cod that weighs between 2.5 and 6.5 kg yields 14.25 NOK per kilogram; cod that weighs between 1.0 and 2.5 kg yields 12.25 NOK per kilogram; and all cod that weighs less than 1.0 kg yields 9.25 NOK per kilogram. Table S3 shows the emerging properties of different fishing mortalities and the NPV for a constant price (NPV_{CP}) and for weight-dependent prices (NPV_{WP}). For comparison, we also show the NPV derived from the model used in the main text. We find that our earlier results presented in Table 1 fully carry over to the case where the price is constant or weight-dependent. Still, evolution increases the NPV of a fishery if fishing mortality is low, and it decreases the NPV of a fishery if fishing mortality is high (Table S4).

Emerging properties for minimum size limits of 25, 45, and 85 cm. Table S5 shows the emerging properties of TAC, total biomass above the age of 3 y, and NPV that complement Fig. 4. For a fishing mortality of $F = 0.8\ y^{-1}$ and a minimum size limit equal to 25 cm, both the evolving and the nonevolving model population go extinct. When harvest pressure is high and the size limit is low (25 cm), the economic losses due to evolution that we see at a size limit of 45 cm disappear. The NPV values are overall lower, however, for the 25-cm size limit than for the 45-cm size limit. At a very high minimum size of 85 cm, the nonevolutionary model performs insignificantly better than the evolutionary model, suggesting that economic losses from evolutionary change are not increasing as minimum sizes increase. Instead, those evolutionary costs are highest (albeit still small) for a minimum size of 45 cm—a size that is based on historic values for the Norwegian and Russian cod fisheries (4, 21) and very close to the size currently used as a legal minimum size (45). Fig. S2 shows the final genetic trait values (year 2100) for different fishing mortalities ($F = 0.4$, $0.8\ y^{-1}$) and for different minimum size limits. We find here that the evolutionary change is larger as fishing mortality increases for all traits except for growth, and that higher minimum size limits result in lower selective pressure and less evolution (Fig. S2).

Varying the coefficients of genetic variation and fishing mortality. In the evolutionary version of our model, the coefficient of genetic variation (Table S1) has been determined empirically by matching trends in age and length at maturation over a 74-y period (1932–2005) (4). The genetic changes emerging from this study are found to be lower than what has been predicted in comparable studies (1, 7–9). These studies assumed a coefficient of genetic variation for all traits equal to 8% and 6%, respectively. As a robustness check, we therefore used these higher coefficients of genetic variation (6% and 8%) and performed simulations for different fishing mortalities. After fishing with a particular fishing mortality from 1932 to 2100, we compare the simulation endpoints for age at maturation and TAC with our calibrated evolutionary model (Table S1) and nonevolutionary model (for which all coefficients of genetic variation are equal to zero). As expected, we find that an assumed $CV_{z,G}$ of 6% and 8% results in predicting larger evolutionary responses, causing a much lower age at maturation in the year 2100 (Fig. S3*A*). As genetic variance increases, the fish mature at a younger age and at a smaller size, and also grow faster. As fishing mortality increases, age at maturation also declines for the nonevolutionary model, which is entirely due to phenotypic plasticity and density dependence in response to a lower abundance of the stock. For the case where the coefficients of genetic variation are set to 6% and 8%, we find that for a given fishing mortality, higher TACs can be obtained compared with the models where evolutionary change is weaker or even absent. This finding indicates that stronger evolutionary forces tend to have as positive effect on the TAC, and corroborates our earlier finding that evolution toward faster growth tends to have positive effects on the fishery.

1. Dunlop ES, Heino M, Dieckmann U (2009) Eco-genetic modeling of contemporary life-history evolution. *Ecol Appl* 19(7):1815–1834.
2. Huse G, Johansen GO, Bogstad L, Gjosaeter H (2004) Studying spatial and trophic interactions between capelin and cod using individual-based modelling. *ICES J Mar Sci* 61(7):1201–1213.
3. Scheffer M, Baveco JM, Deangelis DL, Rose KA, Vannes EH (1995) Super-individuals a simple solution for modeling large populations on an individual basis. *Ecol Modell* 80(2-3):161–170.
4. Eikeset AM, Dunlop ES, Heino M, Stenseth NC, Dieckmann U (2010) Is evolution needed to explain historical maturation trends in Northeast Atlantic cod? PhD thesis (University of Oslo, Oslo).
5. Eikeset AM, et al. (2013) A bio-economic analysis of harvest control rules for the Northeast Arctic cod fishery. *Mar Pol* 39:172–181.
6. Mousseau TA, Roff DA (1987) Natural selection and the heritability of fitness components. *Heredity (Edinb)* 59(Pt 2):181–197.
7. Dunlop ES, Baskett ML, Heino M, Dieckmann U (2009) Propensity of marine reserves to reduce the evolutionary effects of fishing in a migratory species. *Evol Appl* 2(3): 371–393.
8. Enberg K, Jorgensen C, Dunlop ES, Heino M, Dieckmann U (2009) Implications of fisheries-induced evolution for stock rebuilding and recovery. *Evol Appl* 2(3):394–414.
9. Enberg K, Jørgensen C, Mangel M (2010) Fishing-induced evolution an changing reproductive biology of fish: The evolution of steepness. *Can J Fish Aquat Sci* 67(10): 1708–1719.
10. Roughgarden J (1979) *Theory of Population Genetics and Evolutionary Ecology: An Introduction* (Macmillan, New York).
11. Dieckmann U, Heino M (2007) Probabilistic maturation reaction norms: Their history, strengths, and limitations. *Mar Ecol Prog Ser* 335:253–269.
12. Heino M, Dieckmann U, Godø OR (2002) Reaction norm analysis of fishery-induced adaptive change and the case of the Northeast Arctic cod. *ICES CM Series*, Report Y: 14. Available at http://brage.bibsys.no/imr/handle/URN:NBN:no-bibsys_brage_3050.
13. International Council for the Exploration of the Sea (ICES) (2008) *Report of the Arctic Fisheries Working Group*, ICES CM 2008/ACOM:01 (ICES, Copenhagen).
14. Gunderson DR, Dygert PH (1988) Reproductive effort as a predictor of natural mortality-rate. *J du Conseil* 44(2):200–209.
15. Lester NP, Shuter BJ, Abrams PA (2004) Interpreting the von Bertalanffy model of somatic growth in fishes: The cost of reproduction. *Proc Biol Sci* 271(1548):1625–1631.
16. Thorsen A, Kjesbu OS (2001) A rapid method for estimation of oocyte size and potential fecundity in Atlantic cod using a computer-aided particle analysis system. *J Sea Res* 46(3-4):295–308.
17. Kjesbu OS, Witthames PR, Solemdal P, Walker MG (1998) Temporal variations in the fecundity of Arcto-Norwegian cod (*Gadus morhua*) in response to natural changes in food and temperature. *J Sea Res* 40(3-4):303–321.
18. McEvoy LA, McEvoy J (1992) Multiple spawning in several commercial fish species and its consequences for fisheries management, cultivation and experimentation. *J Fish Biol* 41(Suppl B):125–136.
19. Beverton RJH, Holt SJ (1957) On the dynamics of exploited fish populations. *Fish Investment Series 2* (UK Ministry of Agriculture, Fisheries and Food, London), Vol 19.
20. Hylen A (2002) Fluctuations in abundance of Northeast Arctic cod during the 20th century. *ICES Mar Sci Symp* 215:543–550.
21. International Council for the Exploration of the Sea (ICES) (2009) *Report of the Arctic Fisheries Working Group*, ICES CM 2009/ACOM:2 (ICES, Copenhagen).
22. Bochkov YA (1982) Water temperature in the 0–200m layer in the Kola-Meridian in the Barents Sea, 1900–1981. *Sb Nauchn Trud PINRO* 46:113–122, Russian.
23. Tereshchenko VV (1996) Seasonal and year-to-year variations of temperature and salinity along the Kola meridian transect. Report CM 1996/C:11 (Intl Council for the Exploration of the Sea, Copenhagen).
24. Hjermann DO, et al. (2007) Food web dynamics affect Northeast Arctic cod recruitment. *Proc Biol Sci* 274(1610):661–669.
25. Ottersen G, Hjermann D, Stenseth NC (2006) Changes in spawning stock structure strengthens the link between climate and recruitment in a heavily fished cod stock. *Fish Oceanogr* 15(3):230–243.
26. Yaragina NA, Bogstad B, Kovalev YA (2009) Variability in cannibalism in Northeast Arctic cod (*Gadus morhua*) during the period 1947–2006. *Mar Biol Res* 5(1):75–85.
27. Billerbeck JM, Lankford TE, Jr., Conover DO (2001) Evolution of intrinsic growth and energy acquisition rates. I. Trade-offs with swimming performance in *Menidia menidia*. *Evolution* 55(9):1863–1872.
28. Nicieza AG, Metcalfe NB (1999) Costs of rapid growth: The risk of aggression is higher for fast-growing salmon. *Funct Ecol* 13(6):793–800.
29. Walters CJ, Juanes F (1993) Recruitment limitation as a consequence of natural selection for use of restricted feeding habitats and predation risk-taking by juvenile fishes. *Can J Fish Aquat Sci* 50:2058–2070.
30. Biro PA, Post JR (2008) Rapid depletion of genotypes with fast growth and bold personality traits from harvested fish populations. *Proc Natl Acad Sci USA* 105(8): 2919–2922.
31. Bjordal Å, Gjøsæter H, Mehl S (2004) Management strategies for commercial marine species in northern ecosystems. *Proceedings of the 10th Norwegian–Russian Symposium*. Norwegian Institute of Marine Research (IMR)/Polar Research Institute of Marine Fisheries and Oceanography (PINRO) Joint Report Series 1. Available at www.imr.no/filarkiv/2004/12/Imr-Pinro-1-2004.pdf/nb-no.
32. Richter AP, Eikeset AM, Van Soest DP, Stenseth NC (2011) Towards the optimal management of the Northeast Arctic cod fishery. *Fondazione Eni Enrico Mattei Working Paper 591*. Available at www.feem.it/userfiles/attach/20115201140194NDL2011-040.pdf.
33. Clark CW (1990) *Mathematical Bioeconomics: The Optimal Management of Renewable Resources* (Wiley, New York), 2nd Ed.
34. Grafton RQ, Kompas T, Hilborn RW (2007) Economics of overexploitation revisited. *Science* 318(5856):1601.
35. Norwegian Directorate of Fisheries (2009) Profitability survey on the Norwegian fishing fleet (Norwegian Directorate of Fisheries, Bergen, Norway). Available at www.ssb.no/a/english/aarbok/tab/tab-370.html.
36. International Council for the Exploration of the Sea (ICES) (2008) Report of the ICES Advisory Committee. *ICES Advice 2008* (ICES, Copenhagen).
37. Bogstad B, et al. (2005) Harvest control rules for management of fisheries on Cod and Haddock and optimal long term optimal harvest in the Barents Sea ecosystem. *Report of the Basic Document Working Group (BDWG) to the Joint Norwegian–Russian Fisheries Commission*. Available at www.regjeringen.no/upload/kilde/fkd/prm/2005/0084/ddd/pdfv/262877-vedlegg_11_bdwg-2005_final.pdf.
38. Kovalev YA, Bogstad B (2005) Evaluation of maximum long-term yield for Northeast Arctic cod. *Ecosystem Dynamics and Optimal Long-Term Harvest in the Barents Sea*

Fisheries, ed Shibanov V (Norwegian Institute of Marine Research/Polar Research Institute of Marine Fisheries and Oceanography, Murmansk, Russia), pp 1–18.
39. Marshall CT, Needle CL, Thorsen A, Kjesbu OS, Yaragina NA (2006) Systematic bias in estimates of reproductive potential of an Atlantic cod (*Gadus morhua*) stock: Implications for stock-recruit theory and management. *Can J Fish Aquat Sci* 63(5):980–994.
40. Urbach D, Cotton S (2008) Comment: On the consequences of sexual selection for fisheries-induced evolution. *Evol Appl* 1(4):645–649.
41. Hutchings JA, Rowe S (2008) Response: On the consequences of sexual selection for fisheries-induced evolution. *Evol Appl* 1(4):650–651.
42. Hutchings JA, Rowe S (2008) Consequences of sexual selection for fisheries-induced evolution: An exploratory analysis. *Evol Appl* 1(1):129–136.
43. Food and Agricultural Organization of the United Nations (FAO) (1998) *Introduction to Tropical Fish Stock Assessment. Part 1: Manual*. FAO Fisheries Technical Paper (FAO, Rome).
44. Norwegian Fishermen's Sales Organization (2010) Minimum price list. Circular no. 2010/16 (Norwegian Fishermen's Sales Organization, Tromsø, Norway). Norwegian.
45. International Council for the Exploration of the Sea (ICES) (2012) *Report of the Arctic Fisheries Working Group* (ICES, Copenhagen).

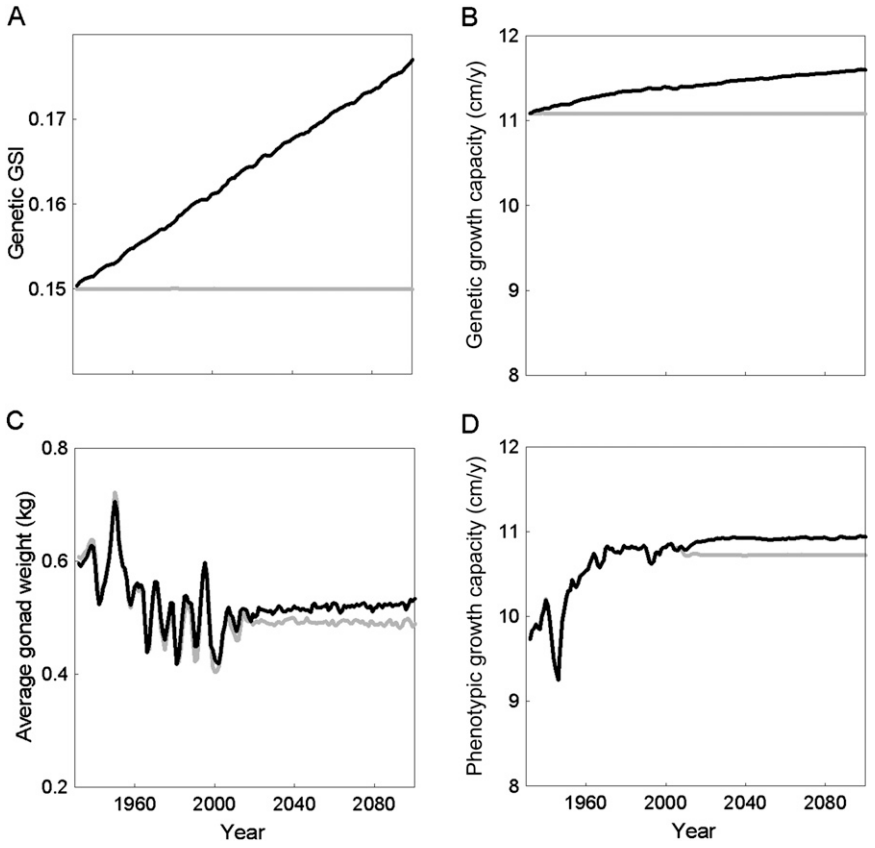

Fig. S1. Life-history changes from 1932 to 2100 in the scenario with historic fishing pressure for the evolutionary (black lines) and nonevolutionary model (gray lines), corresponding to Figs. 2 and 3. (*A*) Genetic gonadosomatic index (GSI), (*B*) genetic growth capacity, (*C*) average gonad weight, and (*D*) phenotypic growth capacity.

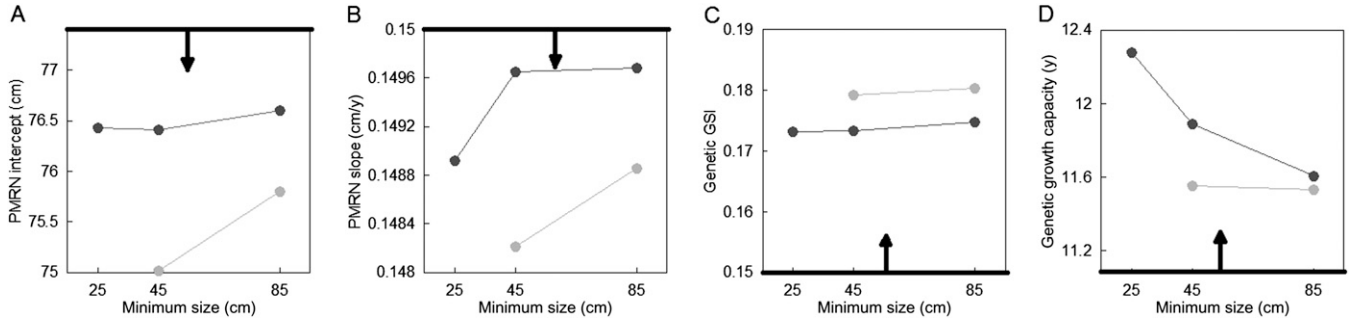

Fig. S2. Predicted evolved life-history traits at the simulation endpoints in the year 2100 for different minimum size limits and different fishing mortalities. Fishing mortalities were applied from 1932 to 2100. Results shown are for the evolutionary model. Coefficients of genetic variation are the same as those used in the main text. Initial trait values are shown by the horizontal bold line, and the arrow shows the direction of evolution. Dark-gray lines and circles are for $F = 0.4\ y^{-1}$, and light-gray lines and circles are for $F = 0.8\ y^{-1}$. (*A*) Probabilistic maturation reaction norm (PMRN) intercept, (*B*) PMRN slope, (*C*) genetic gonadosomatic index (GSI), and (*D*) genetic growth capacity.

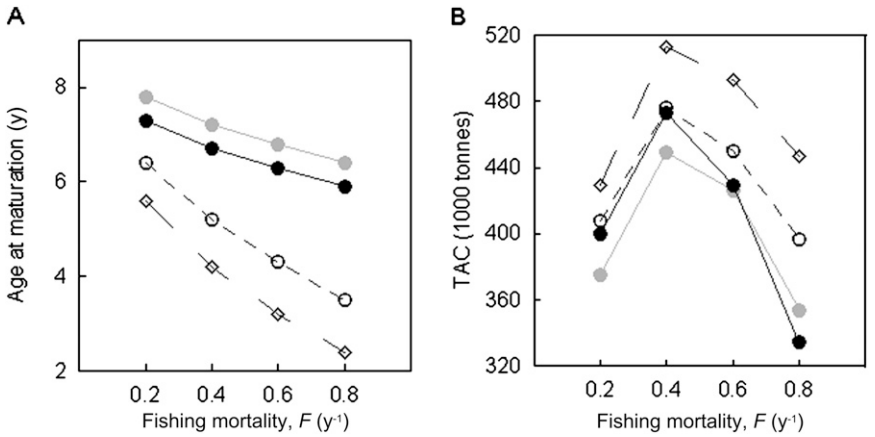

Fig. S3. Predicted stock characteristics at the simulation endpoints in the year 2100 for different coefficients of genetic variation, $CV_{z,G}$, and different fishing mortalities, *F*. Fishing mortalities were applied from 1932 to 2100. Open circles are for $CV_{z,G}$ = 6% for all traits, and open squares are for $CV_{z,G}$ = 8% for all traits; gray circles are for the nonevolutionary model, and black circles are for the evolutionary model used in the main text (Table S1). (*A*) Age at maturation and (*B*) total allowable catch (TAC).

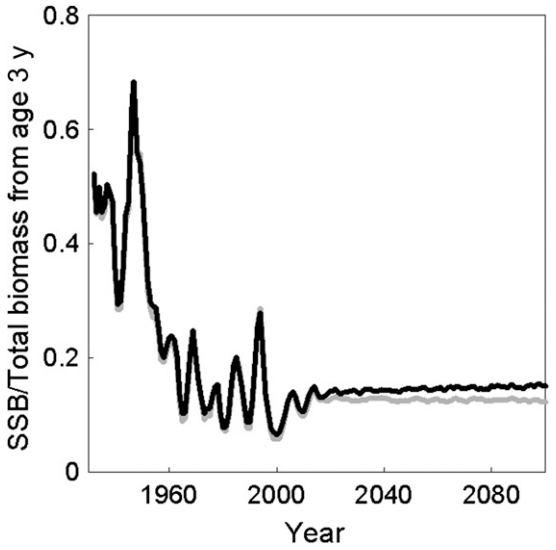

Fig. S4. Ratio between spawning stock biomass (SSB) and total biomass from age 3 y in the scenario with historic fishing pressure for the evolutionary (black line) and nonevolutionary model (gray line).

Table S1. Parameter values and data sources for the bioeconomic model

Parameters	Value	Source
Biological model component		
Initial mean PMRN slope, $\bar{s}_G$	0.15 cm y^{-1}	4, 12
Initial mean PMRN intercept, $\bar{i}_G$	77.4 cm	4, 12
Initial mean reproductive investment, $\overline{GSI}_G$	0.15	17
Initial mean growth capacity, $\bar{g}_G$	11.08 cm	4, 5, M. Heino*
PMRN width, w	12.88 cm	4, 12
Coefficient of genetic variation in PMRN slope, $CV_{s,G}$	10%	4
Coefficient of genetic variation in PMRN intercept, $CV_{i,G}$	2%	4
Coefficient of genetic variation in reproductive investment, $CV_{GSI,G}$	12%	4
Coefficient of genetic variation in genetic growth, $CV_{g,G}$	4%	4
Initial heritability, h_z^2	0.2	6
Strength of density dependence in growth, x	2.08 10^{-5} kg^{-1}	4, 5, M. Heino*
Reproductive investment conversion factor, γ	0.60241	14
Allometric constant, k	3.2 10^{-6} kg cm^{-j}	O. S. Kjesbu*
Allometric exponent, j	3.24	O. S. Kjesbu*
Weight-specific oocyte density, D	4.45 10^6 kg^{-1}	16
Maximal growth capacity, g_{max}	105 cm	4
Stock recruitment constant, c_1	0.7549 kg^{-1}	4, 20, 21
Density-dependent stock recruitment constant, c_2	–6.0633 kg^{-1}	4, 20, 21
Temperature coefficient in stock recruitment, c_0	0.4241 $°C^{-1}$	PINRO**, 22, 23
Natural mortality probability, m	0.18	21
Immature fishing probability in spawning grounds pre-1932	0.38	M. Heino*, O. R. Godø*
Immature fishing probability in feeding grounds pre-1932	0.09	M. Heino*, O. R. Godø*
Minimum size limit on feeding grounds	45 cm	21, O. R. Godø*
Economic model component		
Intercept of the demand function, b_0	18.88 NOK kg^{-1}	32
Slope of the demand function, b_1	1.19 10^{-8} NOK kg^{-2}	32
Stock–output elasticity, α	0.58	32
Effort–output elasticity, β	0.85	32
Catchability coefficient, q	6.17 10^{-4} $tonnes^{-1}d^{-1}$	32
Fixed costs per boat, c_f	1.55 10^6 NOK	32
Variable costs per boat, c_v	131.6 NOK $tonnes^{-1}d^{-1}$	32
Optimal number of tonnage days, e*	66,712 tonnes/d	32

Economic data for the Northeast Arctic cod fishery: costs and harvests from the Norwegian Directorate of Fisheries, Bergen, Norway, provided by P. Sandberg; biomass and total landings are from ICES (21); and demand function is from Statistics Norway, Oslo, Norway, and Norwegian Directorate of Fisheries. Economic values have been inflation corrected using the Producer Price Index from the Organisation for Economic Cooperation and Development, Paris, France, with year 2000 as a baseline. The applied exchange rate is 1 US dollar = 5.6 NOK. Biological data for the Northeast Arctic cod stock is described below.
*IMR, Institute of Marine Research, Bergen, Norway: Survey data on growth from 1932 to 2009 provided by M. Heino; allometric data from survey 1999–2007 provided by O. S. Kjesbu; data on fishing mortality and minimum size limit provided by M. Heino and O. R. Godø.
**PINRO, Knipovich Polar Research Institute of Marine Fisheries and Oceanography, Murmansk, Russia: Temperature data.

Table S2. Optimal HCR with parameters F_{max}, B_{max}, and corresponding NPV for different discount rates (δ), 0%, 2%, and 4%

Model	δ, %	F_{max}	B_{max}	F	TAC	SSB	NPV
Evolution	0	0.33	100	0.33	467 (60)	801 (163)	96.0
	2	0.34	20	0.34	469 (60)	767 (163)	25.4
	4	0.35	20	0.35	470 (60)	735 (155)	12.6
Ecology	0	0.33	40	0.33	439 (48)	670 (125)	94.7
	2	0.35	100	0.35	443 (48)	643 (118)	25.3
	4	0.36	100	0.36	445 (48)	618 (114)	12.6

Averages of fishing mortality (F), total allowable catch (TAC), and spawning stock biomass (SSB) with temporal SDs in parentheses. Units: F_{max} and F (y^{-1}); B_{max}, TAC, and SSB (1,000 tonnes); NPV (in billions, US dollars). HCR, harvest control rule; NPV, net present value.

Table S3. Averages for different constant fishing mortalities from 1932 to 2100, showing TAC, total biomass from age 3 y, and NPV for a discount rate of 2% assuming NPV_{CP} and NPV_{WP}

F	Model	TAC	Biomass	NPV_{CP}	NPV_{WP}	NPV
0.2	Evolution	400 (55)	2,686 (375)	25.7	30.5	23.1
0.2	Ecology	375 (42)	2,503 (277)	24.6	29.2	23.0
0.4	Evolution	473 (60)	1,779 (216)	27.3	31.5	25.2
0.4	Ecology	449 (51)	1,711 (178)	26.47	30.8	25.1
0.6	Evolution	429 (70)	1,208 (176)	21.41	23.8	21.6
0.6	Ecology	427 (66)	1,246 (164)	22.1	24.8	22.3
0.8	Evolution	335 (90)	800 (191)	13.0	13.9	14.7
0.8	Ecology	354 (85)	889 (176)	15.10	16.6	16.7

For comparison we also show the NPV derived from the model used in the main text. Temporal SDs for total allowable catch (TAC) and biomass are shown in parentheses. Units: *F* (y^{-1}); TAC and total biomass (1,000 tonnes); NPV (in billions US dollars). NPV_{CP}, net present value for constant price; NPV_{WP}, net present value for weight-dependent prices.

Table S4. Mean values corresponding to the historic fishing pressure in Fig. 2

Model	*F*	TAC	SSB	Biomass	NPV
Evolution	0.68	360 (95)	267 (365)	1,103 (562)	17.8
Ecology	0.68	370 (93)	260 (356)	1,167 (526)	18.6

Averages of fishing mortality (*F*), total allowable catch (TAC), total biomass from age 3 y, and spawning stock biomass (SSB) with temporal SDs in parentheses, and finally net present value (NPV). The NPV is given for a discount rate of 2%. Units: *F* (y^{-1}); TAC, biomass, and SSB (1,000 tonnes); NPV (in billions, US dollars).

Table S5. NPV, TAC, and total biomass from age 3 y for the minimum size limits 25, 45, and 85 cm across different constant fishing mortalities, *F*

	Minimum size (cm)					
	25		45		85	
	Evolution	Ecology	Evolution	Ecology	Evolution	Ecology
TAC						
F = 0.2	337 (48)	310 (34)	400 (154)	375 (42)	222 (50)	215 (54)
F = 0.4	325 (58)	283 (49)	473 (60)	449 (51)	336 (65)	331 (55)
F = 0.6	217 (79)	170 (79)	429 (69)	426 (66)	401 (70)	398 (60)
F = 0.8	—	—	335 (91)	354 (86)	441 (71)	446 (67)
NPV						
F = 0.2	20.7	20.2	23.1	23	13.4	12.9
F = 0.4	16.9	15.5	25.2	25.1	19.1	19.7
F = 0.6	6.4	4.51	21.6	22.3	22.0	22.8
F = 0.8	—	—	14.7	16.7	23.6	24.5
Biomass						
F = 0.2	2,026 (309)	1,852 (221)	2,689 (374)	2,505 (276)	3,914 (535)	3,833 (479)
F = 0.4	1,034 (191)	896 (159)	1,778 (216)	1,709 (178)	3,639 (446)	3,590 (446)
F = 0.6	487 (183)	385 (184)	1,208 (176)	1,245 (165)	3,464 (395)	3,438 (423)
F = 0.8	—	—	798 (193)	888 (178)	3,341 (365)	3,324 (382)

Values shown for total allowable catch (TAC) and total biomass (1,000 tonnes) are averages for 1932–2100 with temporal SDs in parentheses. The net present value (NPV) (in billions, US dollars) is given for a discount rate of 2%. Units: *F* (y^{-1}); TAC and total biomass (1,000 tonnes); NPV (in billions, US dollars).